# Robust Anti-Windup Control Design for PID Controllers–Theory and Experimental Verification

**Payam Kheirkhahan**[1*]

[1]Department of Electrical Engineering, Garmsar branch, Islamic Azad University, Garmsar, Iran
*Email of Corresponding Author: kheirkhahan_payam@hotmail.com
*Received: October3, 2017; Accepted: December 10, 2017*

**Abstract**
This paper addresses an approximation-based anti-windup (AW) control strategy for suppressing the windup effect caused by actuator saturation nonlinearity in proportional–integral–derivative (PID) controlled systems. The effect of actuator constraint is firstly regarded as a disturbance imported to the PID controller. The external disturbance can then be modeled by a linear differential equation with unknown coefficients. Using Stone-Weierstrass theorem, it is verified that these differential equations are universal approximators. An auxiliary control signal is finally designed to modify the error signal injected to the PID controller. The proposed AW control scheme is simple, system independent and applicable by digital or analog circuits. Analytical studies as well as experimental results using MATLAB/SIMULINK external mode, demonstrate high performance of the proposed approach. It is shown that the proposed AW scheme renders the performance of the controlled system more robust toward the effects of windup than conventional PID AW schemes. The stability analysis is provided by Lyapunov's second method.

**Keywords**
Back Calculation, Conditional Integration, Limited Integrator, Preloading, Realizable Reference, Universal Approximator

## 1. Introduction

Practical systems have some constraints owing to physical restriction of the actuators [1]. What specially is investigated here is the physical limitations associated with actuator saturation. Because of this phenomenon, the actual input of the plant may differ from the controller output in practice. If saturation is not properly taken into consideration in the control design, the results can be disastrous such as performance degradation, overshoot, and undershoot as well as instability in the closed-loop response of control systems due to a well-known phenomenon called windup effect [2]. Therefore, many papers have been published and are related to the stability of control input saturation [3-6].
The wind-up problem was originally considered in using PI and PID controllers for controlling linear systems where an integrator in the error path causes a persistent increase in the control signal until actuator saturation occurs. In order to weaken the effect of windup, two basic solutions have been reported in the literature. One approach is to consider the limitations on actuators as parts of the plant and use nonlinear control theory for the design procedure. However, the control scheme obtained in this manner is unsuitable and imposes many unnecessary complexities to the problem, while the simplicity of implementation should be maintained as a basic feature [7]. Another approach is to first ignore actuator saturation and design a linear controller that meets the

performance specifications, and then design an anti-windup compensator to handle adverse effects of the input saturation. This method was widely used in control engineering and there are many techniques for designing an anti-windup compensator [8-10].

In order to avoid the windup phenomena, some anti-windup strategies have already been developed and significant progress has been reported in the literature. Anti-windup control methodology is a popular approach to saturation control. The objective of all anti-windup control schemes is to stabilize the system, and to recover as much performance as possible of the system in the presence of the saturation. This two-step design procedure has several distinct advantages. First, it separates the requirement of stability and performance from saturation control. When designing the nominal controller without regarding saturation, the designer is free to choose different control design approaches as desired. If this proves to be insufficient in the face of actuator saturation, then a compensator can be added. Therefore, this approach alleviates the inherent complication involved in the design of saturation compensators.

Many solutions to the anti-windup problem have been given in some papers. It is impossible to list all of these, but comprehensive summaries of these methods can be found in [11-12] and references therein. A general solution was described in [13]. The idea is to use an observer which can take into account some saturation on the control variable. As windup was originally observed in Proportional-Integral (PI) and PID controllers designed for SISO control systems with a saturating actuator, Anti-reset windup which has also been referred to as back-calculation and integrator resetting was introduced [14] to cope with. A general framework that unifies a large class of existing anti-windup control schemes in terms of two matrix parameters was proposed in [15]. This framework is useful for understanding different anti-windup control schemes and motivates the development of systematic procedures for designing anti-windup controllers that provide guaranteed stability and performance. Popov stability condition was applied to the anti-windup compensator design problem in [16]. However, the synthesis condition is given in coupled Riccati equations, which is difficult to solve. Alternatively, by modeling the saturation as a sector-bounded nonlinearity, the synthesis conditions of static and dynamic anti-windup controllers were formulated as LMI problems in [17-20] using extended Circle Criterion. This approach was to recast the design of anti-windup compensator as a robust $H_\infty$ problem.

Walgama and Sternby developed an observer-based anti-windup compensator [21]. Niu designed a robust anti-windup controller based on the Lyapunov approach to accommodate the constraints and disturbance [22]. Another solution namely, the conditioning technique was derived in [23, 24]. The idea is computing the realizable reference variables that would just have produced the actual control variables. The original version of the conditioning technique is restricted to the case where the controller has no time delay. In [25], a modified version of the conditioning technique was introduced for a multivariable controller with a general time-delay structure. One drawback in the conditioning technique was addressed in [26] using an adaptive approach. [27, 28] is also developed an adaptive anti-windup compensator. In the case of adaptive control, it should be noted that computation requirements for real-time parameter identification and sensitivity to numerical accuracy and the existing noise increase in an undesirable form as the state variables increases.

Moreover, they are unable to handle unstructured uncertainty and external disturbances, which are missing link in almost all the proposed approaches [29].

To tackle these problems, Neural-Network based AW control design has been proposed. The universal approximation property has been an important motivation for this widespread application of fuzzy systems and neural networks [30-31]. Many improvements have been reported, but the main idea which is estimating and compensating the uncertainties using the universal approximation property of neural networks and fuzzy systems has been remained unchanged. Fault-tolerance, parallelism and excellent learning capabilities are other beneficial characteristics of fuzzy systems and neural networks [32]. Although these controllers have been practically successful, their design procedure is not strain forward. In adaptive fuzzy control, there are many tuning parameters such as the center and width of the Gaussian membership functions and also the weight of each rule. Usually, these parameters are adjusted online using the adaptation laws derived from stability analysis. Nevertheless, the initial values of these parameters and their convergence rate are important issues that considerably affect the controller performance and should be selected carefully [33].

Widespread applications of PID controllers in industry and the fact that they are usually experience windup phenomenon motivate us to discuss some of anti-windup approaches in this research. As an extension in this field, differential equation is utilized to approximate actuator nonlinearity in the controller. An auxiliary control signal is then designed and presented to modify the error signal injected to the PID controller. The uniformly ultimately boundedness of all the control signals is guaranteed through rigorous Lyapunov analysis. The experimental results demonstrate that the proposed controller can effectively suppress the actuator saturation nonlinearity and offers superior control performance despite the existence of control input constraints.

The rest of this paper is organized as follows. In section 2, PID control design is reviewed. Section 3 presents some of conventional anti-wind-up methods considering actuator voltage input limitation. Section 4 presents the proposed model-free anti-windup control design. Stability analysis and performance evaluation are discussed in section 5. Section 6 is dedicated to the experimental results of a level control system which has been constructed in laboratory. Finally, section 7 concludes the paper.

## 2. PID Control Design

Although many efficient approaches for controller design have emerged in the last decade, PID controllers are still the most common controllers in industry, since the benefit-cost ratio obtained by these controllers is not achievable easily by the other controllers [3, 34]. Continuous time PID controllers have been studied extensively [35-37]. However, in practical applications, their performance is limited by actuator saturation and thus, followed by integrator wind-up. Let a dynamic system be controlled by a PID controller $K(s)$ as shown in Figure 1:

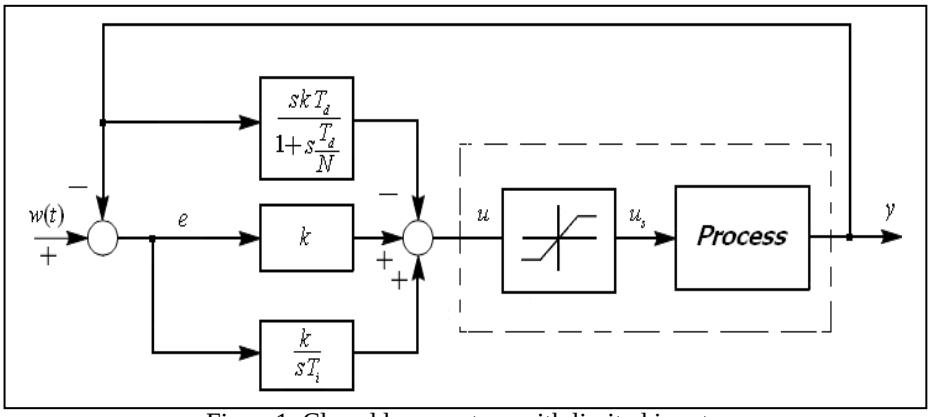


Figure1. Closed loop system with limited input

$$K(s) = k_p + \frac{k_i}{s} + k_d s \tag{1}$$

Where $k_p, k_i$, and $k_d$ are the proportional, integral and derivative constants of the controller, respectively. The PID controller, $K(s)$ can be described in a time constant form as follows [3]:

$$K(s) = k\left[1 + \frac{1}{T_i s} + T_d s\right] \tag{2}$$

In which $T_i$, and $T_d$ are integral time constant, and derivative time constant, respectively, or in a modified form as

$$K(s) = k\left[1 + \frac{1}{T_i s} + \frac{T_d s}{1 + T_d s / N}\right] \tag{3}$$

Where derivative term is replaced by a filter in order to attenuate the high gain effect induced by high-frequency measurement noise, and N is usually between 7 and 15. It is assumed that the input limitation is described as

$$u_s = sat(u) = \begin{cases} u_{\max} & ;u > u_{\max} \\ u & ;u_{\min} \le u \le u_{\max} \\ u_{\min} & ;u < u_{\min} \end{cases} \tag{4}$$

Where $u$ the controller is output, $u_s$ is the actual process input and $sat(\square)$ denotes the saturation function. As it is obvious from Equation (4), when actuator saturation happens, the actual input of the system is different from the controller output. In this situation, if the controller continues its operation based on the initial design in linear range, the performance of the closed-loop system deviates from the prospected linear performance and consequently the wind-up phenomenon occurs. To describe this phenomenon, it can be assumed that both the process and the controller are in steady state. A positive step change in reference signal $w(s)$ causes a jump in the control signal and leads to actuator saturation at high limit (if $k > 0$). Thus, $u_s$ becomes smaller than $u$ and $y$ will

change less slowly than the system response with unlimited input. Since $y$ is changing slowly $e = w - y$ reduces slowly and the increase in the integrator term is greater than its increase for the unlimited case. When $y$ reaches to $w(s)$, due to the large integral term, $u$ remains saturated or close to the saturation mode. After a sufficiently long time that the error remained negative for a long time, $u$ reduces. These behaviors lead to a large settling time and a large overshoot in the process output. To tackle this problem, some conventional anti-windup control strategies are reviewed in the next section.

## 3. Conventional Anti-Windup Strategies

### *3.1 Limited Integrator*

Limited integrator is a very simple approach to reduce integrator wind-up effects. In this approach, as shown in Figure 2, the integrator input is reduced by feeding back the integrator output via a high-gain dead-zone. In order to utilize the whole linear range of the actuator, the dead-zone region and the linear range of the actuator should be the same. When the integrator value is out of dead-zone band, a feedback signal with the amplitude of Equation 4 is produced to affect the integrator input.

$$f = b(i(t) - H') \tag{5}$$

In (5), $H'$ is a dead-zone band, $b$ is dead-zone gain and $i(t)$ is the integrator value. If $b$ is selected large $(b > 10)$, the integrator output is limited to $H'$ effectively.

### *3.2 Back-Calculation*

Back-calculation (tracking anti-windup) is a conventional method to prevent integrator wind-up. The TAW standard structure used in the literature is shown in Figure 3 in which $T_t$ is the tracking time-constant. When the controller output exceeds the actuator permitted range, integrator input is reduced by feeding back the difference between the saturated and unsaturated control signals. It should be mentioned that the saturation block shown in Figure3 may represent the real saturation in actuator (if actuator-output is measurable) or describe an applied model in the controller. If the

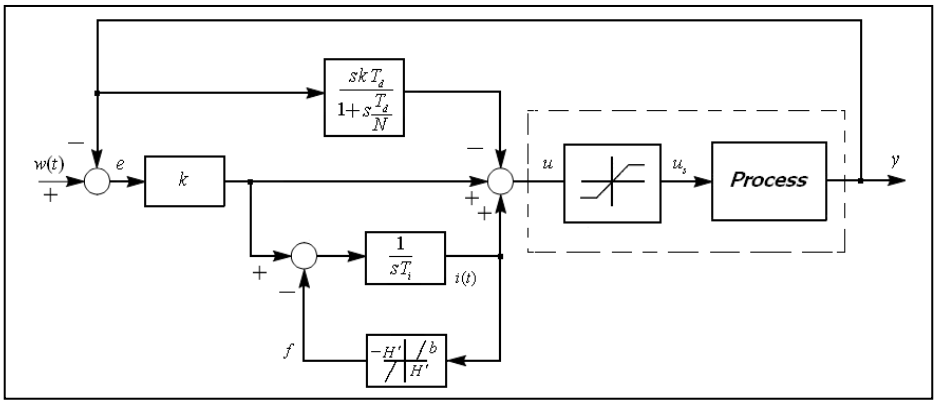


Figure2. PID control with limited integrator

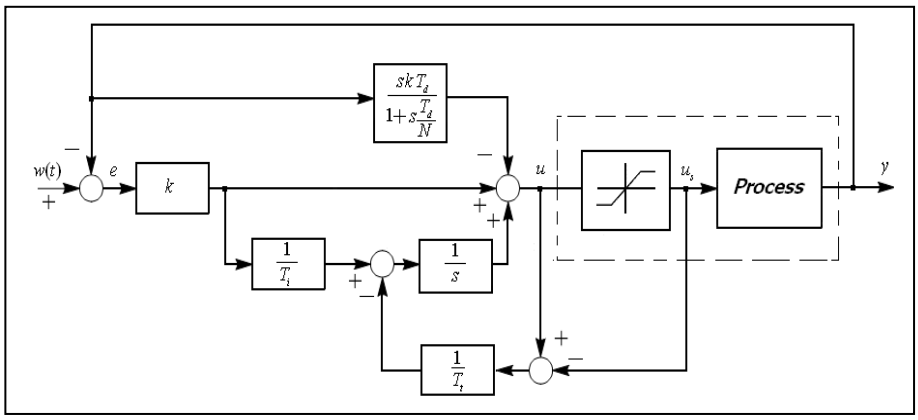


Figure3. PID control with Tracking Anti-Windup

Actuator is described by linear dynamics with saturation part; the problem is that the controller output and so the speed of actuator response will be limited. To solve this problem, the structure shown in Figure3 is changed to the structure in Figure 4 where an unlimited control signal is applied to the process and feedback signal is produced using dead-zone. It should be mentioned that $H'$ denotes the linear range of the actuator and the relationship between $T_t$ and dead-zone gain is described as

$$b = T_i / T_t \qquad (6)$$

A rule of thumb for tuning $T_t$ is $T_t = T_i$ which equivalent is to $b = 1$. However, it has been proven that the larger values of $b$ in special conditions result in a more suitable performance.

*3.3 Modified Tracking Anti-Windup*

Simulation results imply that tracking control is sensitive to variations in $T_t$ and $b$ . Choosing very high value for $b$ can reduce overshoot effectively, while it can lead to slow response. So in this section, the proposed structure in [38] is generalized for PID controllers (Figure 5)

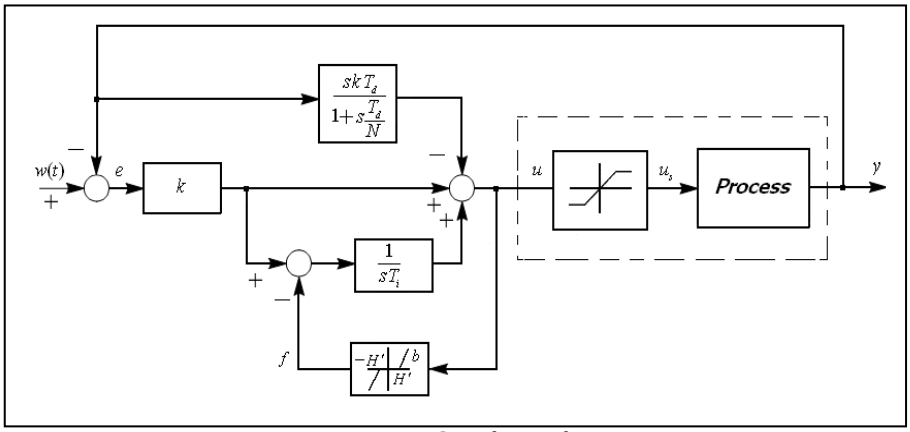


Figure4. Equivalent form of Figure3

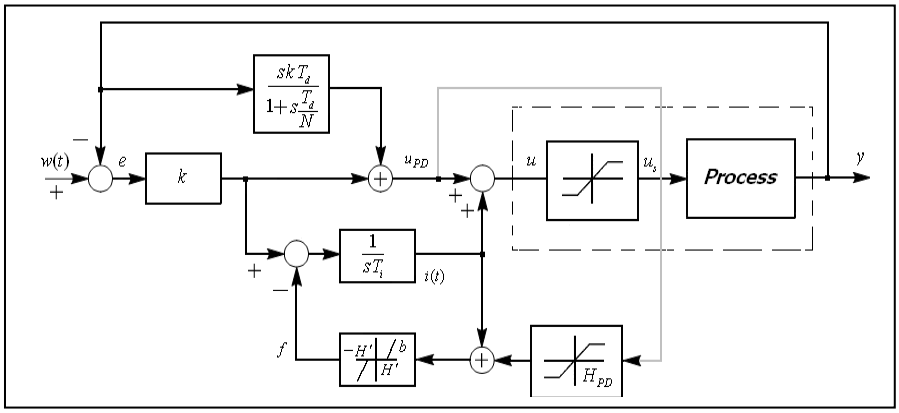


Figure5. Modified Tracking Anti-Windup

The reason of slow response is that a very large initial controller output which is originated from large proportional gains and derivative operations, leads to a large feedback signal for high gain '$b$'.This feedback signal forces the integrator to high negative values, so the controller output comes back to linear operation region. As time goes by, proportional and derivative terms of the control signal decrease. However, the integrator output will not increase rapidly to compensate this reduction. As a result, the controller output becomes very small or even negative. To avoid this, an extra limitation is applied on the proportional-derivative part of the control signal to produce anti-windup feedback signal which makes selection of high gains possible for $b$ i.e. $b=10$. The effect of this additional saturation actuator can be interpreted in this way that if the integrator value exceeds from $\max(H'-u_{PD}(t), H'-H_{PD})$, a feedback signal is applied with the amplitude of

$$f = b(i(t)+\min\{H_{PD}, u_{PD}(t)\}-H') \tag{7}$$

This feedback signal reduces the integrator input and so stops integration action. Normal integration is done only when Equation (8) is satisfied,

$$-H'-\max\{-H_{PD}, u_{PD}(t)\} < i(t) < H'-\min\{H_{PD}, u_{PD}(t)\} \tag{8}$$

In which $u_{PD}$ is the proportional-derivative part of the control signal. In other words, it is limited dynamically to $\max(H'-u_{PD}(t), H'-H_{PD})$. By an extra limitation, a new design parameter is added. In simulations, the ratio $r = H_{PD}/H'$ is used. The suitable range for $r$ is [0.5,1.5]. The choice $r=1$ can be interpreted as continuing integration until the controller signal consisted of the proportional-derivative part, $u_{PD}$, comes back to linear operational range and restarting the integration. Consequently, integrator will not go to negative values and the slow behavior of the step response with a high gain for dead-zone will be prevented.

If the amplitude of the step inputs is large in comparison with the saturation level (70% to 100%), the system response is not sensitive to variations of the parameter $r$. However, for step inputs with small amplitude, choosing small values for $r$ such as $r \in [0.5,1]$ leads to faster response with large overshoot, and choosing larger values for $r$ in the interval [1,1.5] yields in reduced overshoot; although it makes the controlled system response sluggish.

*3.4 Realizable References*

In this method, controller output $u$ originated from applying the realizable reference signal $w_s$ to the controller equals to real system input, $(u_s)$, which is obtained from applying reference signal $w$ to the controller. If the $w_s$ described in Figure 3 is applied, the saturation block will be deactivated ($u_s$ is always similar to $u$) and so the saturation block can be eliminated according to Figure 6. In addition, the signals $u_s$ and $y$ illustrated in this figure are equal to the signals $u_s$ and $y$ illustrated in Figure 3, respectively. As depicted in Figure 6, any nonlinear term has been excluded from the proposed scheme. In fact, the nonlinear term has been included in the reference signal $w_s$. As shown in Figure 6, the output $y$ tracks $w_s$ instead of $w$ with the expected linear performance. Using realizable reference definition, it is obvious that

$$u_s = k\left(1+\frac{1}{T_i s}\right)w_s - k\left(1+\frac{1}{T_i s}+\frac{T_d s}{1+T_d s/N}\right)y \tag{9}$$

This can be rewritten as

$$w_s = \frac{s^2 T_i T_d\left(1+\frac{1}{N}\right)+s\left(T_i+\frac{T_d}{N}\right)+1}{\left(1+sT_i\right)\left(1+\frac{sT_d}{N}\right)}y + \frac{sT_i}{k\left(1+sT_i\right)}u_s \tag{10}$$

Using TAW algorithm, we have:

$$u = k\left(1+\frac{1}{sT_i}\right)w - k\left(1+\frac{1}{sT_i}+\frac{sT_d}{1+\frac{sT_d}{N}}\right)y + \frac{1}{sT_t}\left(u_s-u\right) \tag{11}$$

Subtracting (11) from (9) and after some manipulations, $w_s$ is obtained as

$$w_s = w + \frac{T_i}{kT_t}\frac{1+sT_t}{1+sT_i}(u_s - u) = w + G_w(s)(u_s - u) \tag{12}$$

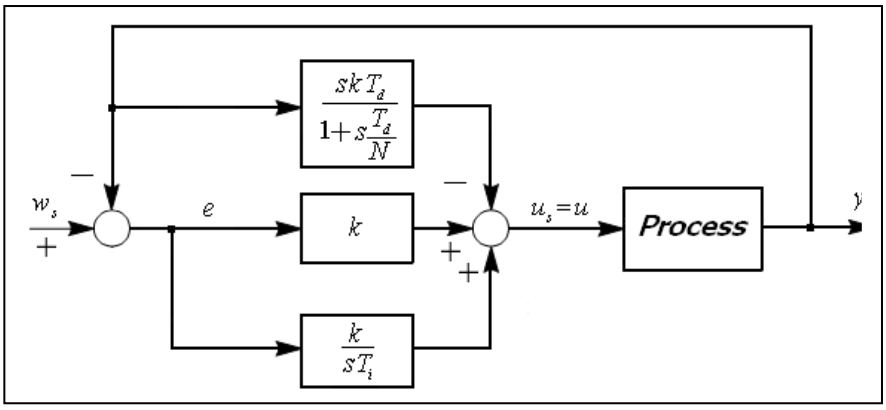


Figure6. Equivalent form of Figure 3

Since $G_w(s)$ is a dynamic transfer function with one zero and one pole, when the controller leaves the limitation and $u_s = u$, $w_s$ is not similar to $w$, unless $G_w(s)$ decreases to a static gain. In fact, when $T_t = T_i$, it follows from Eq. (12) that:

$$G_w(s) = \frac{1}{k} \tag{13}$$

$$w_s = w + \frac{u_s - u}{k} \tag{14}$$

Also, when the controller leaves the limitation, we will have $w_s = w$, which results in the best tracking performance.

*3.5 Conditional Integration*

In this method, the integrator term is increased only when special conditions are met. Otherwise, its value is kept constant. There are various types of conditional integrator characterized as below:

1- The integrator term is limited to a selected value.

2- The integration is stopped when the system error becomes large $(|e| > \bar{e})$ in which $\bar{e}$ is a selected value.

3- The integration is stopped when the controller is saturated.

4- The integration is stopped when actuator saturation occurs and the controller error and control signal $u$ have the same sign $(e \times u > 0)$.

All of these methods have been compared in [39-40], and it has been shown that the scheme 4 outperforms the others.

*3.5.1 Integrator Limiter (CI-ILIM) [41]*

This method imposes a hard limitation (saturation) on the integrator value $\eta$ such that:

$$\dot{\eta} = \begin{cases} 0 & \eta \notin [\eta_{\min}, \eta_{\max}] \ \& \ e.(\eta - \bar{\eta}) > 0 \ , \\ & \bar{\eta} \ \square \ (\eta_{\min} + \eta_{\max})/2 \\ e & o.w \end{cases} \tag{15}$$

The initial challenge of this method is choosing the integrator limits $\eta_{\min}$ and $\eta_{\max}$. In this study, we have selected them as

$$(\eta_{\min}, \eta_{\max}) = (\frac{T_i u_{\min}}{k}, \frac{T_i u_{\max}}{k}) \tag{16}$$

*3.5.2 Conditionally Freeze Integrator (CI-CFRZ)*

In this method when $u$ moves towards saturation, $\dot{\eta}$ is frozen. It means that:

$$\dot{\eta} = \begin{cases} 0 & u \neq u_s \ \ \& \ \ e.(u - u_s) > 0 \\ e & o.w \end{cases} \tag{17}$$

A common strategy related with conditional integration, which is often applied in chemical engineering, is freezing the integrator input to zero when $u$ is saturated.

$$\dot{\eta} = \begin{cases} 0 & u \neq u_s \\ e & o.w \end{cases} \tag{18}$$

Although the integrator value $\eta$ is held constant, leaving the saturation region is not guaranteed in this method.

*3.6 Preloading*

In this method, when the controller output is saturated, the integrator value $(\eta)$ is reset to the predefined value $\eta_d$. In the other words:

$$\dot{\eta} = \begin{cases} -\alpha(\eta - \eta_d) & u \neq u_s \\ e & o.w \end{cases} \tag{19}$$

In which $\alpha > 0$ determines the integrator delay rate during saturation of the control signal $u$. Similar to CI-ILIM method, choosing the design parameter $\eta_d$ is a challenging problem. Also similar to CI-FRZ, leaving the saturation region is not guaranteed in this method.

*3.7 Variable Structure PID Anti-Windup (VSPID)*

In this method, when the nominal control $u$ is in saturation region, the integrator term is driven dynamically such that the control signal $u$ is placed on the edge of the saturation region [42]. As a result, this method removes the defects of previous methods. In this strategy, $\dot{\eta}$ is given by

$$\dot{\eta} = \begin{cases} -\beta T_i (u - u_s)/k & u \neq u_s \ \ \& \ \ e.(u - \bar{u}) > 0 \ , \\ & \bar{u} \ \square \ (u_{\min} + u_{\max})/2 \\ e & o.w \ . \end{cases} \qquad (20)$$

Where $\beta$ is a positive constant and is chosen so that $u$ converges rapidly to the nearest edge of the interval $[u_{\min}, u_{\max}]$ (the settling time in saturation zone is $T_{settle} = \frac{4}{\beta}$). It can be easily verified that if $\beta = \frac{1}{T_t}$ and the switch shown in Figure 7 is replaced with an adder; VSPID will be similar to TAW [42]. Some specifications of this method are as follows.

1- It is possible for designers to apply their knowledge in the field of PID controller design.

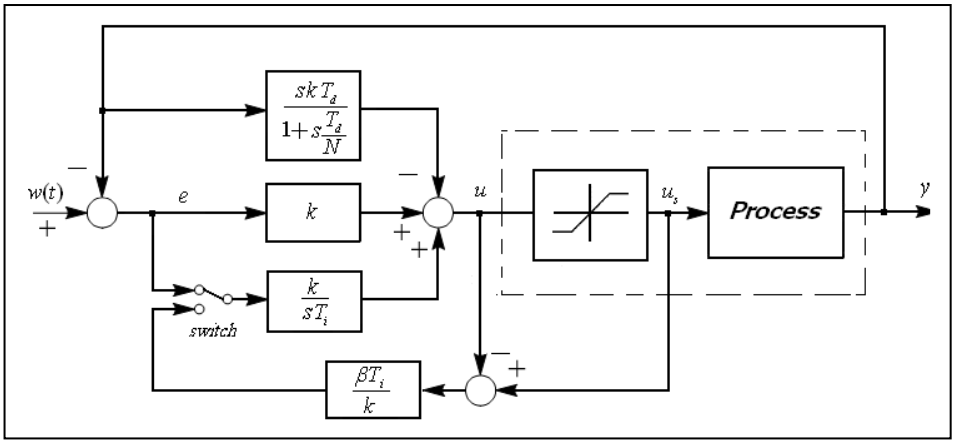


Figure7. Variable structure PID anti-windup

2- The design parameter $\beta$ can be determined using the operational specifications of closed-loop system. As a rule of thumbs, $\beta$ should be selected such that during saturation, integrator feedback loop performs 2-5 times faster than the closed-loop system settling time.

3- Due to the switching behavior of the controller described in (20) and feeding back the saturation error $(u - u_s)$, the control signal $u$ tends to remain near the saturation zone (during actuator saturation). As a result, this controller turns to the linear operational zone faster than the other discussed controllers.

*3.8 Hybrid Method*

Some anti-windup strategies by combining conditional integrator and back-calculation methods have been presented [42-43]. In [43], it has been proposed to apply an extra limitation for proportional-derivative part in order to produce an anti-wind up feedback signal. However, it is

followed by problems associated with tuning extra design parameters. Suppose that a step change from the initial value of $y_0$ to the final value of $y_1$ is required. As mentioned before, integrator wind-up occurs when a step change in $w$ leads to actuator saturation. In this case, the system error reduces slower than ideal case (without actuator saturation) and so the integrator value becomes large. As a result, even when the output $y$ reaches to $w$ , the controller is still in saturation region, due to the integrator term, which leads to large overshoot and long settling time. An important point in these techniques is their deficiency in the presence of dead-time in processes which is undesirable for industrial regulators. The solution is combination of conditional integration and back-calculation method. Back-calculation is applied when the controller is saturated ($u \neq u_s$), system error and the corrected value of $u$ have the same sign ($e \times u > 0$), and the system output has converged to the new set point. In other words:

$$\dot{\eta} = \begin{cases} \dfrac{k}{T_i} e + \dfrac{1}{T_t}(u_s - u) & if \quad u \neq u_s \ \ \& \ \ e \times u > 0 \ \ \& \begin{cases} y > y_0 & \text{if } y_1 > y_0 \\ y < y_0 & \text{if } y_1 < y_0 \end{cases} \\ \dfrac{k}{T_i} e & o.w \end{cases} \tag{21}$$

**Remark 1:** The value of $T_t$ determines the rate of the integration reset and also the performance of the total control scheme. Some of options for selecting $T_t$ are $T_t = T_i$ and $T_t = \sqrt{T_i T_d}$ [39].

## 4 Description of Control Structure

In this section, the subject of model free control is used to establish an anti-windup scheme. Controller with actuator saturation is shown in Figure 8. The actual input of plant is $u_s$ , that is related to $u$ , control signal, by the function "saturation" as shown in Equation (4). Now, the crucial question is that the uncertainty is belonging to the system model or controller equations. As it is known, one explanation of windup phenomena can be stated like this: because of saturation, the actual plant input will be different from the output of the controller, in turn, the controller output does not derive the plant and as a result, the states of the controller are wrongly updated. Therefore, when saturation occurs, the actual controller states are different from desired states. Hence, we can infer that the uncertainty is associated with controller. It should be mentioned that, by considering uncertainty in controller, this approach can be applied to other realizable linear controllers. By using a proper compensator, the error between desired and actual states of controller will converge to zero asymptotically and the closed-loop respond is restored. Equations are rewritten as follows

$$\dot{x}_c = A_c x_c + B_c e \tag{22}$$

$$u_s = C_c x_c + \sigma \tag{23}$$

Where $\sigma$ denotes the actuator's non-implemented control signal as

$$\sigma = sat(u) - u \tag{24}$$

In addition, the desired controller that yields good tracking performance in the absence of saturation nonlinearity, is given by

$$\dot{x}_c^d = A_c x_c^d + B_c e_d \tag{25}$$

$$u_d = C_c x_c^d \tag{26}$$

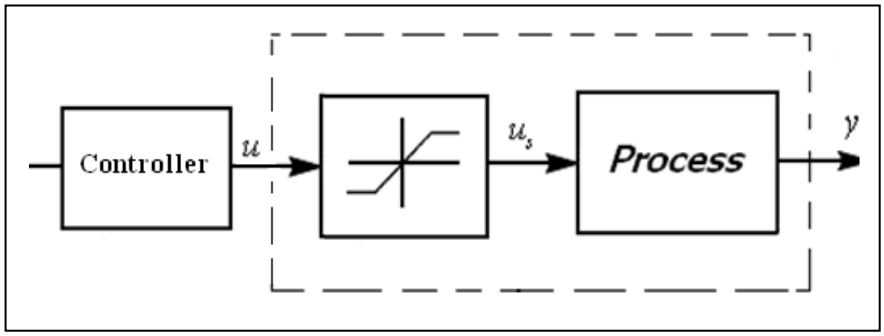


Figure8. System with actuator saturation

This part of the design procedure is quite straightforward and is carrying out independent of saturation nonlinearity. Subtracting (25) from (22) and (26) from (23) yields the error dynamic equations as

$$\dot{E} = A_c E + B_c \aleph \tag{27}$$

$$\zeta = C_c E + \sigma \tag{28}$$

Where

$$E = x_c - x_c^d \quad , \quad \aleph = e - e_d \quad , \quad \zeta = u_s - u_d \tag{29}$$

Now, the problem is to design an algorithm to improve the position error denoted by $e$ so that it can minimize the error of updating states of the controller. With this in mind, the following quantities are defined.

$$\Xi = E^{(p)} - \sum_{j=1}^{p} b_j E^{(p-j)} \tag{30}$$

$$\delta = \aleph^{(p)} - \sum_{j=1}^{p} b_j \aleph^{(p-j)} \tag{31}$$

Where $b_j$ 's are (real) scalars. Differentiating both (27) and (28) with respect to time and using (30) and (31) with the assumption that $\sigma$ can be modeled by a pth order Ordinary Differential Equation (ODE) as [44-47],

$$\sigma^{(p)} = \sum_{j=1}^{p} b_j \sigma^{(p-j)} \tag{32}$$

We have the following results

$$\dot{\Xi} = A_c \Xi + B_c \delta \tag{33}$$

$$\zeta^{(p)} = \sum_{j=1}^{p} b_j \zeta^{(p-j)} + C_c \Xi + \wp(t) \tag{34}$$

Where $\wp(t)$ is the lumped approximation error? It should be noted that, the order *p* reflects the dynamic structure of $\sigma$, which is in most cases considered one or two. Now, we can define a coordinate transformation represented by

$$L = \begin{bmatrix} \zeta & \dot{\zeta} & \dots & \zeta^{(p-1)} & \Xi \end{bmatrix}^T \tag{35}$$

Then, the controller state equation in new coordinates will be

$$\dot{L} = \Lambda L + G\delta + W\wp(t) \tag{36}$$

That $\delta$ is a new control input vector defined as

$$\delta = -\mu L = -\mu_0 \Xi - \sum_{j=1}^{p} \mu_j \zeta^{(p-j)} \tag{37}$$

And

$$\Lambda = \begin{bmatrix} 0 & 1 & 0 & \cdots & 0 & 0 \\ 0 & 0 & 1 & \cdots & 0 & 0 \\ \vdots & \vdots & \vdots & \vdots & \vdots & \vdots \\ 0 & 0 & \cdots & \cdots & 1 & 0 \\ b_p & b_{p-1} & \cdots & \cdots & b_1 & C_c \\ 0 & 0 & \cdots & \cdots & 0 & A_c \end{bmatrix}$$

$$G = \begin{bmatrix} 0 & \cdots & 0 & B_c^T \end{bmatrix}^{\mathrm{T}} \ , \ W = \begin{bmatrix} 0 & 0 & 0 & 1 & 0 \end{bmatrix}^{\mathrm{T}} \tag{38}$$

It must be noted that if $(A_c, B_c)$ is controllable, then $(\Lambda, G)$ is also controllable and finally the error can be forced to zero. Substituting (37) into (36) yields

$$\dot{L} = (\Lambda - G\mu)L + W\wp(t) \tag{39}$$

The remaining task here is to adjust the control input *e* to account for the effects of actuator nonlinearity as follows:

$$e = e_d + \aleph \tag{40}$$

Where $\aleph$ is the auxiliary control input? The last equation says that in order to cope with the windup phenomenon, the error signal injected to linear controller must be changed to (40). A block diagram of the closed loop control system is illustrated in Figure 9.

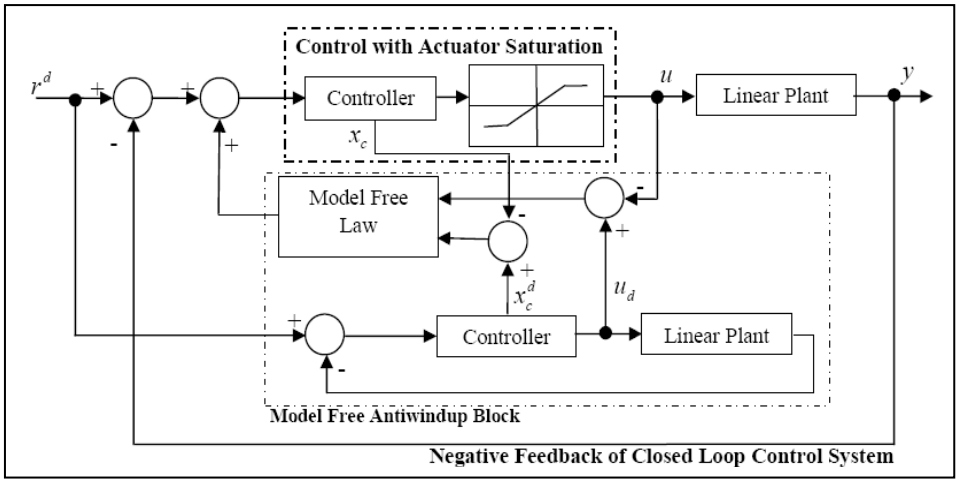


Figure9. The block diagram of the proposed scheme

*Controller Design Steps:*

In short, the overall design procedure can be summarized as follows:

1. The control parameters matrices $A_c$ , $B_c$ , and $C_c$ are selected by trial and played to achieve the best possible transient performance without considering the actuator nonlinearity.
2. The uncertainty is modeled by a pth order ODE.
3. Finally, to implement the proposed control method, the $\mu$ state feedback vector is calculated.

Remark 2: As can be seen, the Eq. (32) is a *p* order ODE. It can be easily shown that the solution of this Equation is a continuous function as:

$$\sigma(t) = \sum_{i=1}^{p} c_i \, e^{\lambda_i t} Cos\left(\omega_i t + \theta_i\right) \tag{41}$$

It is interesting to investigate the capability of the last assumption, Eq. (32), from a function approximation capability point of view. Herein, we will prove that equation (41) has the universal approximation capability. In the following, we suppose that the input universe of discourse *T* is a convex set in $\Re$.

*Proposition1. (Universal Approximation Theorem)*

Let $\sigma(t)$ be a continuous real function on a convex set *T* in $\Re$, then for each arbitrary $\varepsilon > 0$, there exists a function in the form of

$$\sum_{i=1}^{p} c_{\mathrm{i}}\, \mathrm{e}^{\lambda_i t} Cos\left(\omega_i t + \theta_i\right) \tag{42}$$

Such that

$$\underset{t\in T}{Sup}\left|\sum_{i=1}^{p} c_{\mathrm{i}}\, \mathrm{e}^{\lambda_i t} Cos\left(\omega_i t + \theta_i\right) - \sigma(t)\right| < \varepsilon \tag{43}$$

Proof: let Z to be a set of continuous function on *T* convex set in the form of (41) and suppose $\sigma_1(t)$ and $\sigma_2(t)$ are given as [29]

$$\begin{aligned} \sigma_1(t) &= \sum_{i=1}^{p} c_{\mathrm{i}}\, \mathrm{e}^{\lambda_i t} Cos\left(\omega_i t + \theta_i\right) \\ \sigma_2(t) &= \sum_{j=1}^{p} \bar{c}_{\mathrm{j}}\, \mathrm{e}^{\bar{\lambda}_j t} Cos\left(\bar{\omega}_j t + \bar{\theta}_j\right) \end{aligned} \tag{44}$$

We have

$$\sigma_1(t) + \sigma_2(t) = \sum_{i=1}^{p} c_{\mathrm{i}}\, \mathrm{e}^{\lambda_i t}\, Cos\left(\omega_i t + \theta_i\right) + \sum_{j=1}^{p} \bar{c}_{\mathrm{j}}\, \mathrm{e}^{\bar{\lambda}_j t}\, Cos\left(\bar{\omega}_j t + \bar{\theta}_j\right) \tag{45}$$

$$\begin{aligned} \sigma_1(t).\sigma_2(t) = {} & \frac{1}{2}\sum_{i=1}^{p}\sum_{j=1}^{p} c_{\mathrm{i}}\bar{c}_{\mathrm{j}}\, \mathrm{e}^{\left(\lambda_i + \bar{\lambda}_j\right)t}\, Cos\begin{pmatrix} \left(\omega_i + \bar{\omega}_j\right)t \\ +\left(\theta_i + \bar{\theta}_j\right) \end{pmatrix} \\ & + \frac{1}{2}\sum_{i=1}^{p}\sum_{j=1}^{p} c_{\mathrm{i}}\bar{c}_{\mathrm{j}}\, \mathrm{e}^{\left(\lambda_i + \bar{\lambda}_j\right)t}\, Cos\begin{pmatrix} \left(\omega_i - \bar{\omega}_j\right)t \\ +\left(\theta_i - \bar{\theta}_j\right) \end{pmatrix} \end{aligned}$$

Hence, $\sigma_1(t) + \sigma_2(t)$ and $\sigma_1(t).\sigma_2(t) \in Z$ . Finally, for any arbitrary $\gamma \in \Re$ ,

$$\gamma.\sigma(t) = \sum_{i=1}^{p} \gamma c_{\mathrm{i}}\, \mathrm{e}^{\lambda_i t} Cos\left(\omega_i t + \theta_i\right) \tag{46}$$

Which is also in the form of (41) and hence Z is algebra. Therefore, the first condition of Weierstrass theorem is true. We show that Z separates points on *T*. We choose the parameters of the $\sigma(t)$ in the form of (41) as follow

$$c_1 = 1,\ \lambda_1 = -1,\ \omega_1 = 0,\ \theta_1 = 0 \tag{47}$$

Since $t_1 \neq t_2$, then $e^{-t_1} \neq e^{-t_2}$ and therefore the second condition is also verified. To verify the third condition of Weierstrass theorem, we simply observe that any system in the form of (41) with $\omega_{\mathrm{i}} = 0,\ \theta_{\mathrm{i}} = 0$ and $c_i > 0$ has the property that

$$\forall t \in \mathrm{T}\ ,\ \sigma(t) > 0 \tag{48}$$

Hence, Z vanishes at no point of *T*. Thus the three aforementioned conditions are satisfied. Therefore the result follows Stone-Weierstrass Theorem.

## 5. Stability and Performance Analysis

*5.1 Stability Analysis*

Here, we prove stability of the proposed approach which is subject to unstructured uncertainty. Toward this end, consider the following Lyapunov function candidate:

$$V = L^T PL \tag{49}$$

In which $P = P^T$ is a positive definite matrix satisfying the Lyapunov equation $(\Lambda - G\mu)^T P + P(\Lambda - G\mu) = -Q$ where $Q$ is a positive definite matrix. Taking the time derivative of (49) along the trajectories of (39), we have:

$$\dot{V} \le -\lambda_{\min}(Q)\|L\|^2 + 2\lambda_{\max}(P)\|L\|\|\wp(t)\| \tag{50}$$

Where $\lambda_{\min}(Q)$, and $\lambda_{\max}(P)$ denote the minimum and maximum Eigen values of $Q$ and $P$, respectively.

Remark 3: Suppose that the appropriate models are used and the approximation error can be ignored. Then, $\dot{V}$ is negative definite, and the asymptotic stability of $L$ can be approved.

Remark 4: If the approximation error cannot be ignored, after some further manipulations of (50) we have

$$\dot{V} \le \underbrace{-\frac{1}{2}\lambda_{\min}(Q)\|L\|^2}_{c} + 2\frac{\lambda_{\max}^2(P)\|\wp(t)\|^2}{\lambda_{\min}(Q)} \tag{51}$$

We would like to relate (c) to $V$ by considering:

$$V \le \lambda_{\max}(P)\|L\|^2 \tag{52}$$

Now, (51) can be rewritten as

$$\dot{V} \le -\alpha V + \left[\alpha\lambda_{\max}(P) - \frac{1}{2}\lambda_{\min}(Q)\right]\|L\|^2 + 2\frac{\lambda_{\max}^2(P)\|\wp(t)\|^2}{\lambda_{\min}(Q)} \tag{53}$$

Pick $\alpha < \dfrac{\lambda_{\min}(Q)}{2\lambda_{\max}(P)}$, then we have

$$\dot{V} \le -\alpha V + 2\frac{\lambda_{\max}^2(P)\left\|\wp(t)\right\|^2}{\lambda_{\min}(Q)} \tag{54}$$

As a result, $\dot{V} < 0$ whenever

$$V > 2\frac{\lambda_{\max}^2(P)}{\alpha\lambda_{\min}(Q)}\sup_{\tau\ge t_0}\left\|\wp(\tau)\right\|^2 \tag{55}$$

This implies that $(\zeta, \dot{\zeta}, ..., \zeta^{(p-1)}, \Xi)$ is uniformly ultimately bounded.

*5.2 Performance Analysis*

Until now, we have demonstrated the boundedness of the error of the controller output. It should be mentioned that in practical implementations, the transient performance is also of great importance. Solving (54) yields

$$V(t) \le e^{-\alpha(t-t_0)}V(t_0) + 2\frac{\lambda_{\max}^2(P)}{\alpha\lambda_{\min}(Q)}\sup_{t_0\le\tau\le t}\left\|\wp(\tau)\right\|^2 \tag{56}$$

Therefore, according to the lower bound of Lyapunov function, we have

$$\left\|L\right\| \le \sqrt{\frac{V(t_0)}{\lambda_{\min}(P)}}e^{\frac{-\alpha(t-t_0)}{2}} + \sqrt{\frac{2\lambda_{\max}^2(P)}{\alpha\lambda_{\min}(P)\lambda_{\min}(Q)}}\sup_{t_0\le\tau\le t}\left\|\wp(\tau)\right\| \tag{57}$$

That means the tracking error is bounded by a weighted exponential function plus a constant. This also implies that by adjusting the controller parameters, we may improve the tracking error convergence rate. As a consequence,

$$\lim_{t\to\infty}\left\|L\right\| \le \sqrt{\frac{2\lambda_{\max}^2(P)}{\alpha\lambda_{\min}(P)\lambda_{\min}(Q)}}\sup_{t_0\le\tau\le t}\left\|\wp(\tau)\right\| \tag{58}$$

## 6. Real-Time Implementation

*6.1 The Experimental Setup*

In order to evaluate the theoretical methods discussed in previous section, experimental results on a tank manufactured in laboratory are presented. First, the elements of the system are explained. In this research, the studied process is a system consists of four interconnected tanks [48]. Only one of them is used for our experimental objectives. Water is pumped by a “SAM-121108” DC pump with driving voltage of 12V. The computer command is applied to the actuator by a PWM generator circuit and a PCL-818L card (Figure 10). The liquid height is measured using a “Vp441” 100mBar pressure sensor. A current-to-voltage converter circuit is used in order to convert the current signal obtained from the sensor into voltage, for computer calculations. Also, a software-implemented low pass filter with a 5HZ cutoff frequency is used for proper sensor noise attenuation. For real-time implementation, MATLAB Real-Time Windows Target (RTWT) is applied.

*6.2 Experimental Results*

To investigate the effect of integrator windup, the tank described in previous section with PID controller is considered. By using the Zigler-Nicoles method, controller parameters are obtained as:

$$k=60,\quad T_i=5,\quad T_d=1 \tag{59}$$

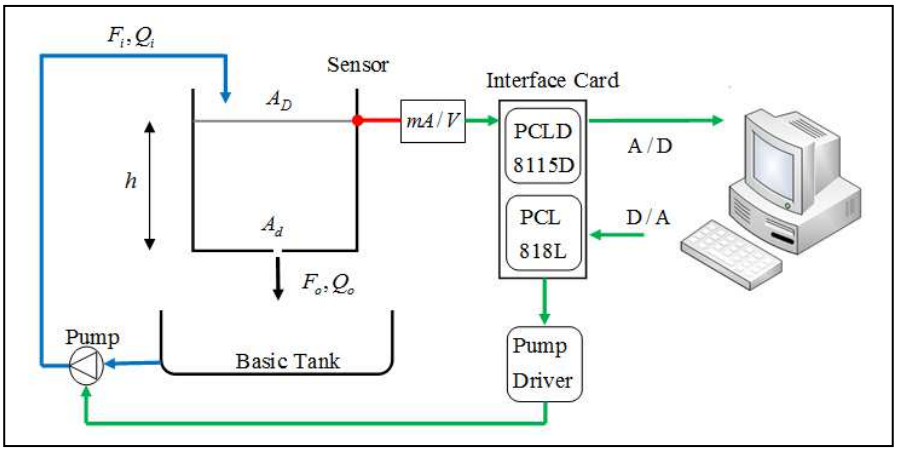


Figure10. The experimental setup

In this research, we have focused on the set-point problem. The initial value of the step reference input is $y_0=1.65$ and its final value has been set to $y_1=1.9$. These values have been selected based on the range of the sensor output current and the desired reference input. Note that for the empty and full tank, sensor output signal after current-to-voltage conversion is 1.65 Volt and 2.5 Volt, respectively. Pump saturation voltage values are set on $u_{\min}=0V$ and $u_{\max}=12V$. The system response to desired input, pump voltage signal and integrator output in the presence of actuator saturation are illustrated in Figure 11. As shown in this figure, the undesirable response stems from control signal saturation and the accumulated error in the integrator (integrator windup). In more details, during saturation, the feedback loop is opened. As a result, an increment in the control signal amplitude does not yield in a faster response by the system. In this situations, if error integration continues, the integrator value increases without any effect on system output. In t=46.1 sec, the system output reaches to set-point value and the error sign changes. However, due to integrator high value, the control signal still remains in saturation region. After this time, integrator output begins its reduction so that in t=98.8 sec, when the error becomes sufficiently negative, the control signal leaves the saturation region which leads to a high overshoot and long settling time. In order to solve this problem and obtain a suitable performance in the presence of actuator saturation, real time implementation of eight conventional anti-windup mechanisms using PID controllers is completed in MATLAB/Simulink environment and their performances are evaluated in this research.

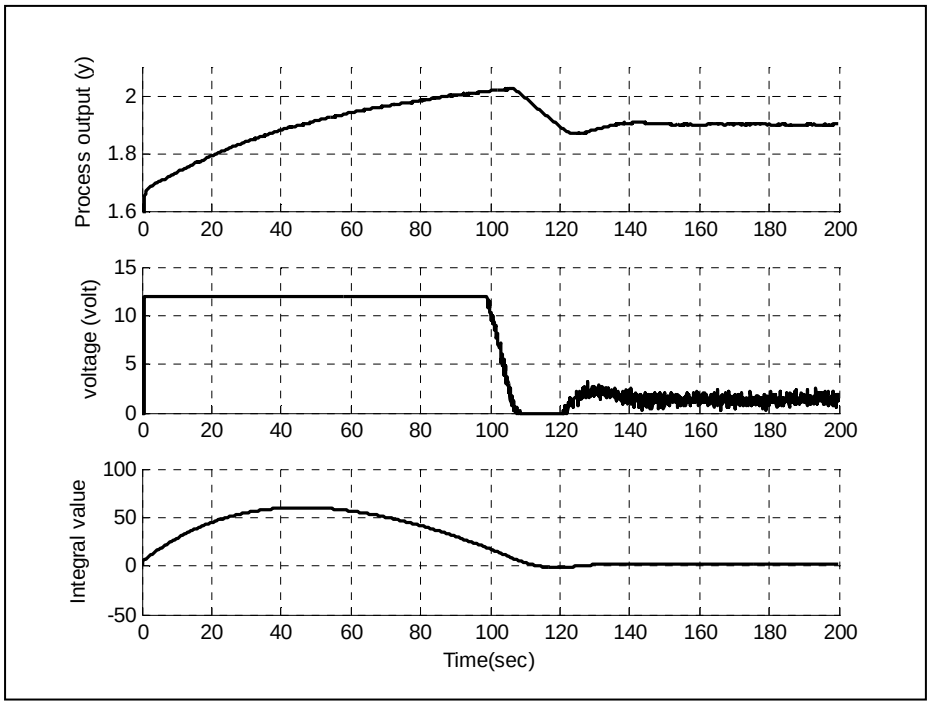


Figure11. System response, Control signal, and Integrator output for conventional PID controller

Limited integrator [49]**:** The system output and pumps voltage signal using 4 different values of $b$ have been depicted in Figure 12. As can be seen, by feeding back the integrator output via a dead-zone element with high gain, its value is limited to the actuator linear range. As a result, the controlled system comes out faster from saturation region and the reduction in settling time and overshoot is obvious.

Tracking Anti-windup method: The system response, pump voltage signal and integrator output in presence of actuator saturation for different values of the parameter $T_t$ are shown in Figure 13. According to this figure, smaller values of $T_t$ obtain more suitable performance (less overshoot and faster exit from saturation).

Modified Tracking anti-windup control: As mentioned before, tracking control method is sensitive to variations of the parameter "$T_t$" and gain "$b$". In other words, choosing small values for $T_t$ reduces the overshoot effectively. In this section, the modified anti-windup tracking controller structure proposed in [38] is investigated for PID controllers. For better understanding the role of added parameter in the design procedure, due to introducing an extra limitation, real-time implementation is repeated for values $b<10$, $b>10$ and also 3 values of $r=0.5,\ 1,\ 1.5$.

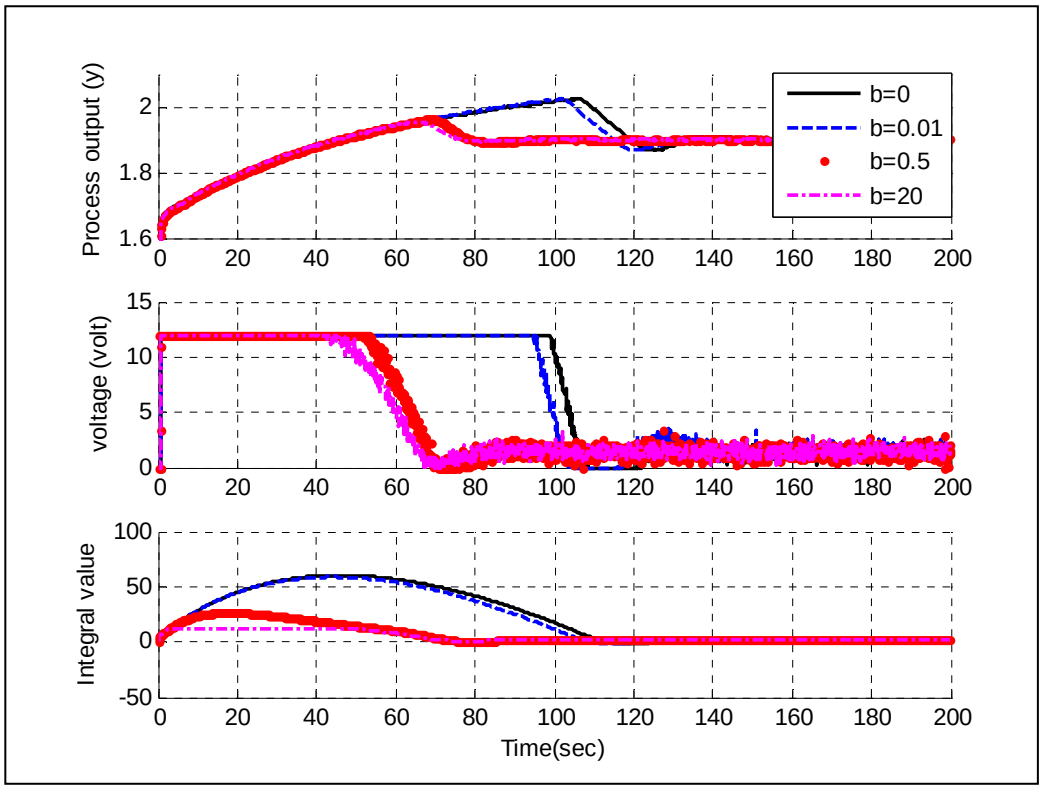


Figure12. System response, Control signal, and Integrator output for limited integrator

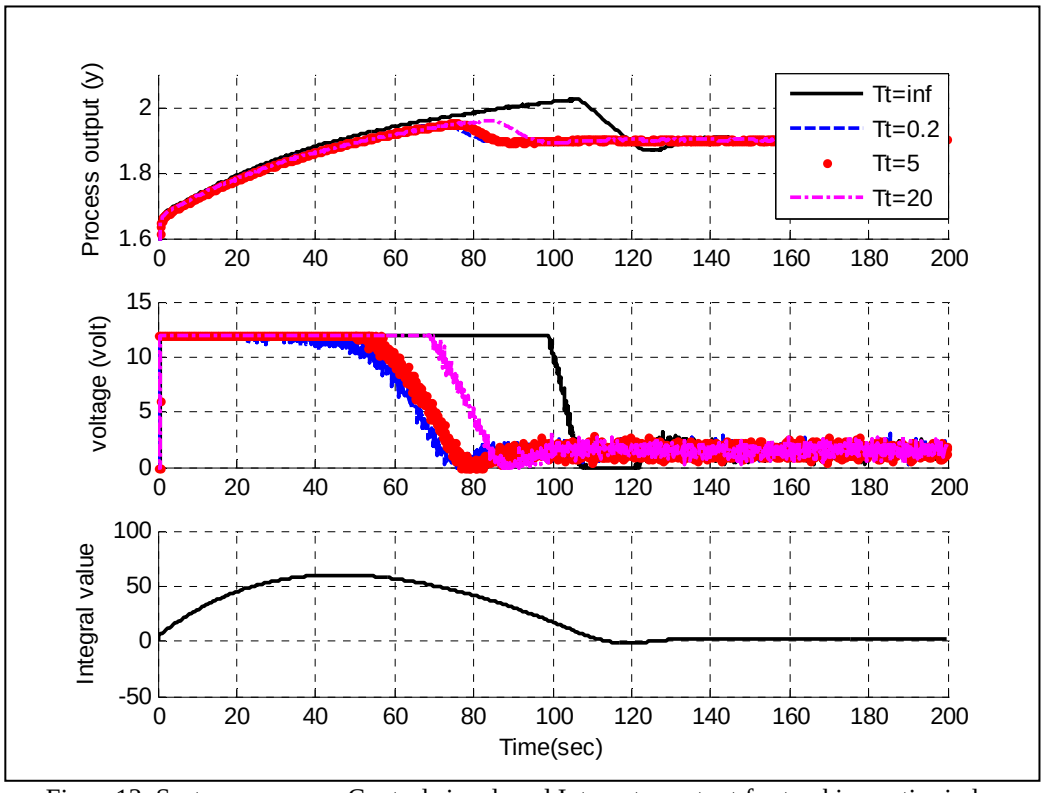


Figure13. System response, Control signal, and Integrator output for tracking anti-windup

A. $b<10$: The system response, pump voltage signal and integrator output in presence of actuator saturation for different values of $r$ are depicted in Figure14. As illustrated in this figure, choosing the parameter $r$ between $r=1$ and $r=1.5$ obtains more satisfactory results.

B. $b>10$: Figure 15 shows the system response, pump voltage signal and integrator output for 3 different values of $r$ and in presence of actuator saturation, respectively. According to Figure 15, a very large initial value for controller output (originated from large proportional gain and derivative operation) results in a large feedback signal with a high gain for $b$ . This feedback signal forces integrator to high negative values until the controller output comes back to linear operational range. As a result, for small values of $r$ , $(r \approx 0.5 \ldots 1)$ , we have a large overshoot, and choosing larger values for $r$ , $(r \approx 1 \ldots 1.5)$ , reduces the overshoot.

Realizable reference: Figure 16 illustrates the closed-loop system response to the realizable reference input in presence of actuator saturation and the integrator output, respectively. The important point is that this method compensates saturation through changing the applied reference signal to closed-loop control system $(w_s)$ .

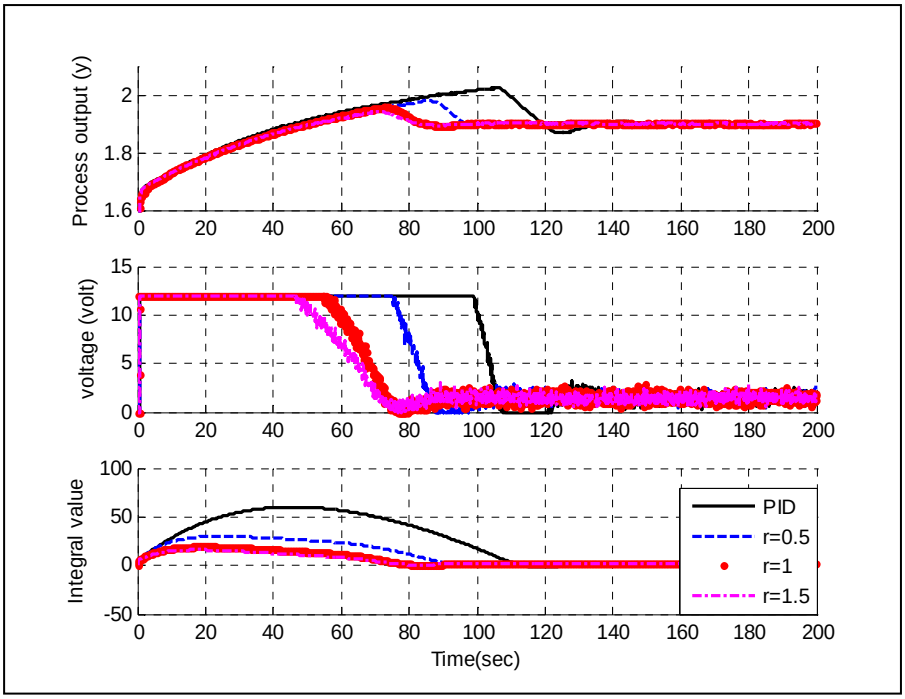


Figure14. System response, Control signal, and Integrator output for modified tracking anti-windup (b<10)

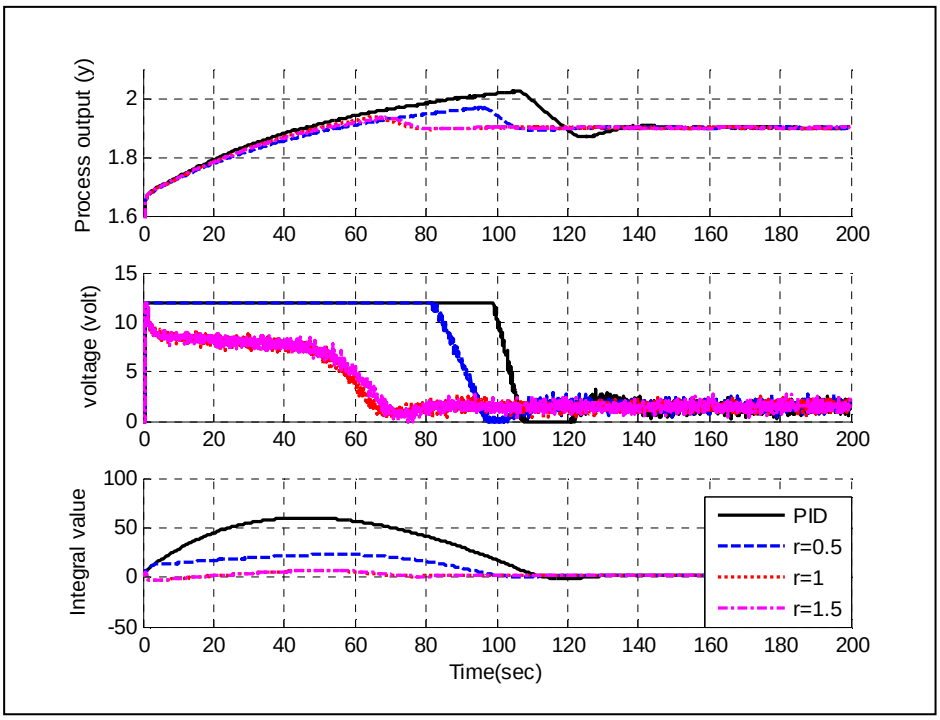


Figure15. System response, Control signal, and Integrator output for modified tracking anti-windup (b>10)

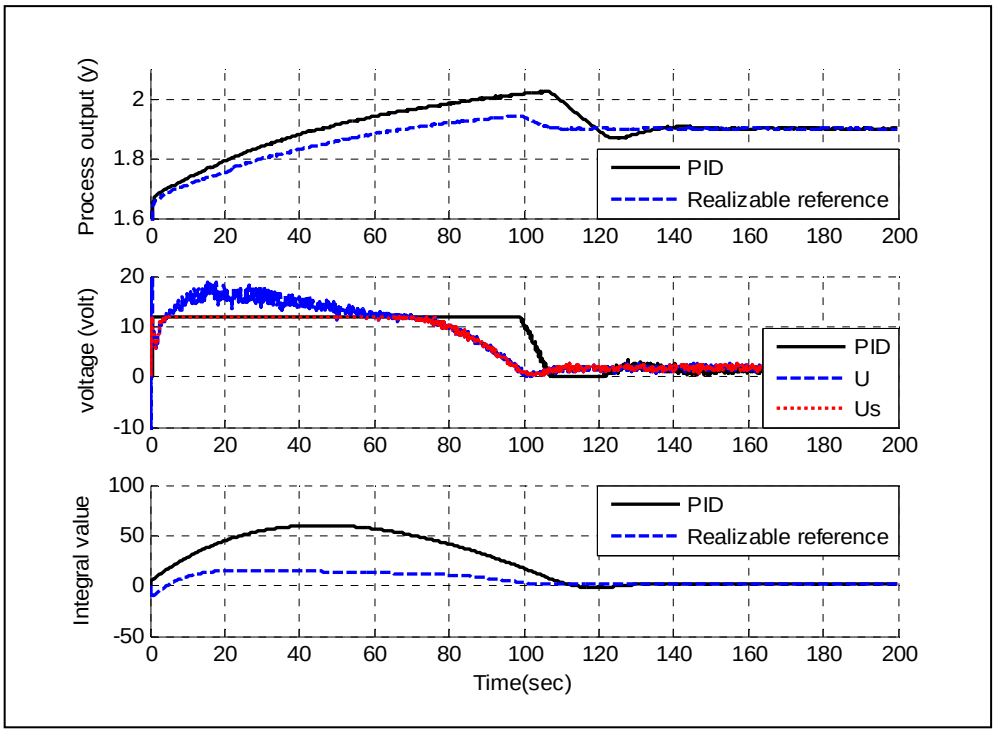


Figure16. System response, Control signal, and Integrator output for realizable reference

Conditional integrator: In this method, integration is switched to one of the situations on or off in specific conditions based on the control signal amplitude or tracking error. In the off case, the integrator initial condition determines its value in that moment. In this section, three methods namely CI-ILIM, CI-CFRZ and CI-FRZ are studied in which the controller parameters are chosen

as $\eta_{\min}=0$ and $\eta_{\max}=1$. The closed-loop system response to desired input, pump voltage signal and integrator term output in the presence of actuator saturation for these methods is illustrated in Figure 17. As shown in these figures, CI-CFRZ and CI-FRZ operate superior than CI-ILIM. It is worthy to mention that in choosing a specific method, the convergence of steady state error to zero should be guaranteed. It means that satisfactory steady state should not be obtained in the absence of integrator.

Preloading: In this approach, the controller parameters have been chosen as $\eta_d=0$ and $\alpha=1$. The closed-loop system response to desired input, pump voltage signal and integrator output is shown in Figure 18.

Variable structure PID anti-windup control: In this section, experimental results for $\bar{u}=6$ and three values of $\beta=0.01, \beta=1$ and $\beta=20$ are shown in Figure19. As illustrated in these figures, the design parameter $\beta$ considerably affects the stability and performance of this method. To be more precise, increasing the gain $\beta$ leads to decreases the settling time and rise time.

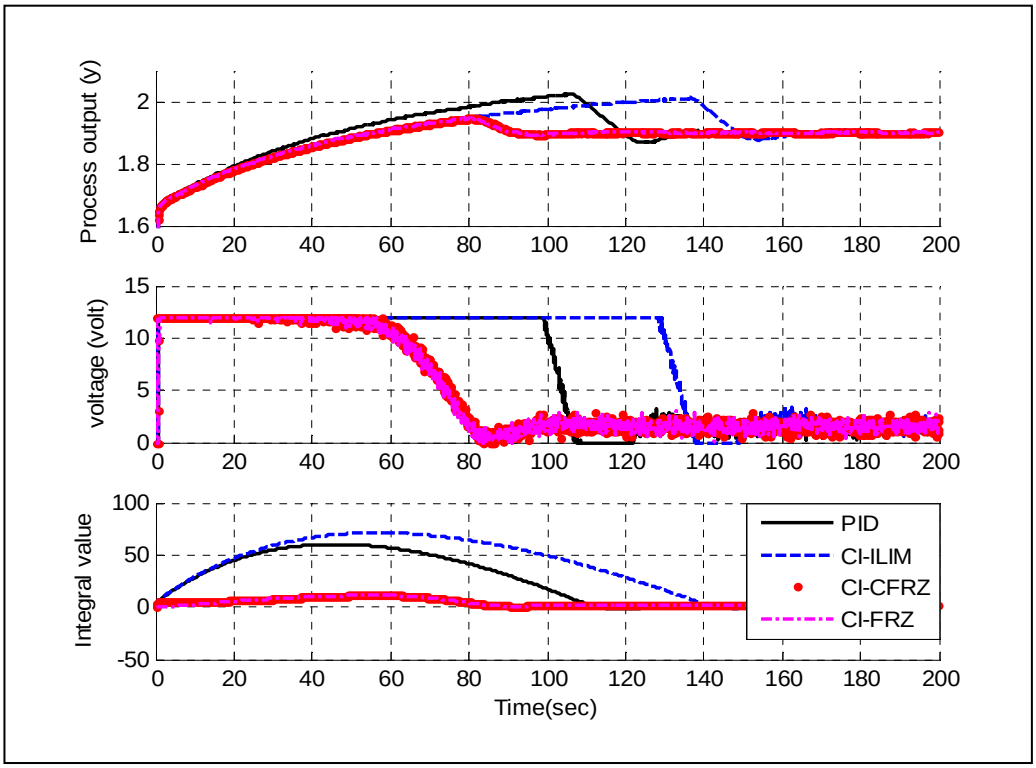


Figure17. System response, Control signal, and Integrator output for conditional integration

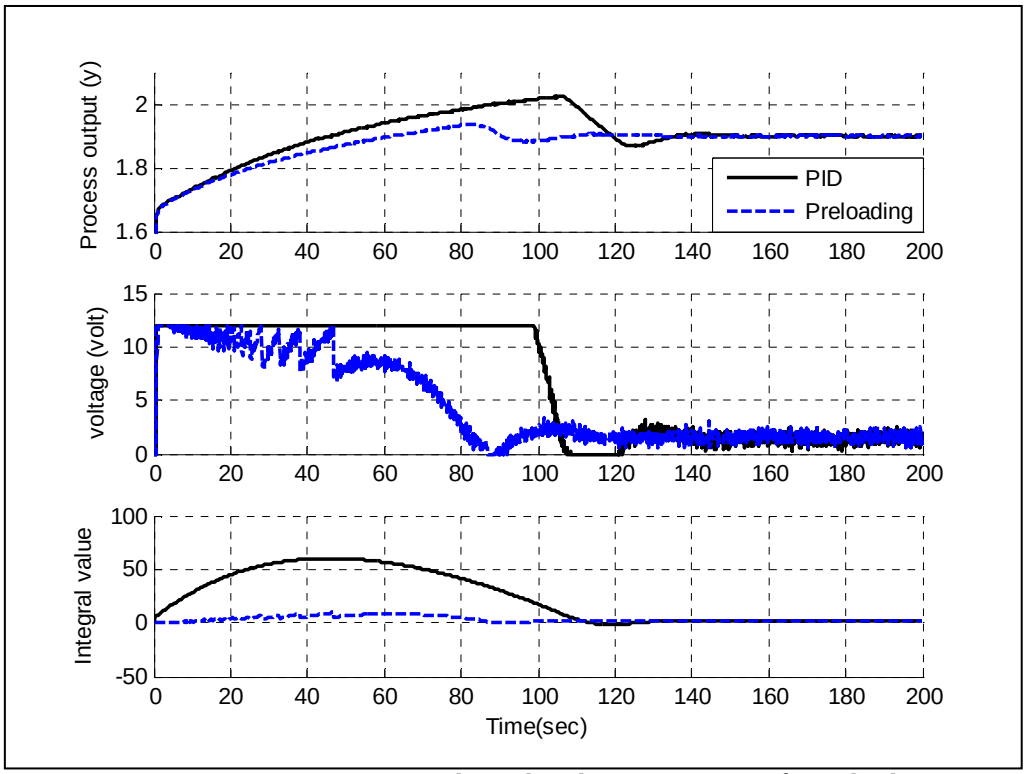


Figure18. System response, Control signal, and Integrator output for preloading

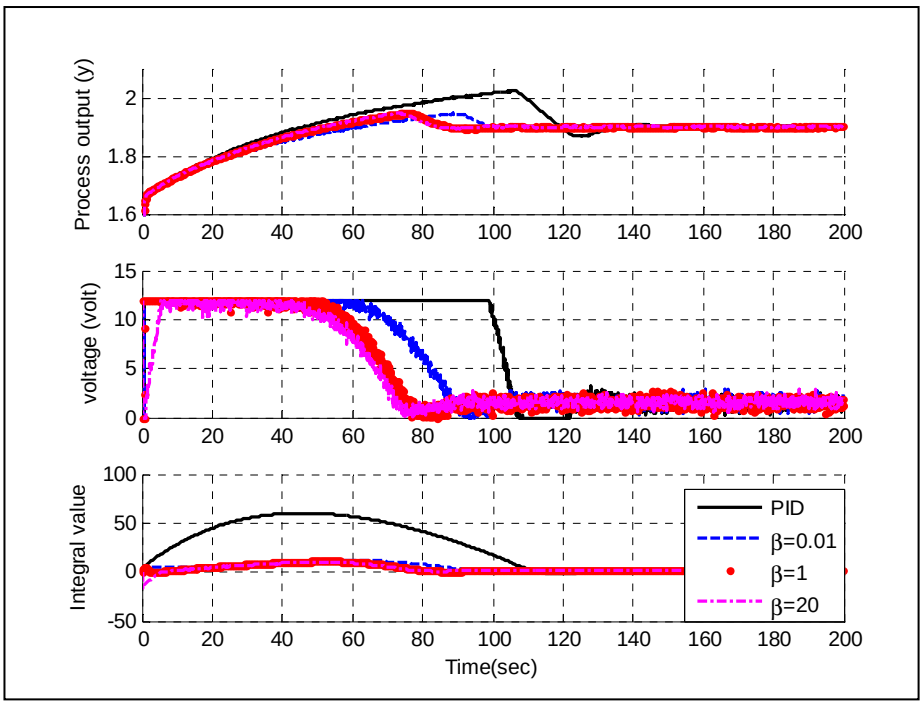


Figure19. System response, Control signal, and Integrator output for variable structure PID

Hybrid method: Figure 20 represents the system response to desired input and pump voltage signal for the proposed scheme by [34] in the presence of actuator saturation. For better evaluation of the results, integrator output for this scheme is also shown in Figure 20. It follows from these figures

that the hybrid method with $T_t = \sqrt{T_i T_d}$ yields in a smaller settling time in the output response and provides better performance in comparison with $T_t = T_i$. This conclusion can be justified simply according to the faster exit of the control signal from saturation region.

Model free AW: Figure21 shows the capability of the proposed approach, under the same control parameters. The non-completed control signal has been modeled by an ordinary differential equation of order 2. For better understanding the control signals are also plotted. From Figure21, it is clear that the control signal of the MFAW leaves the saturation region more rapidly and with a smooth change. One key feature of the proposed method is robustness under parameter variation of the model.

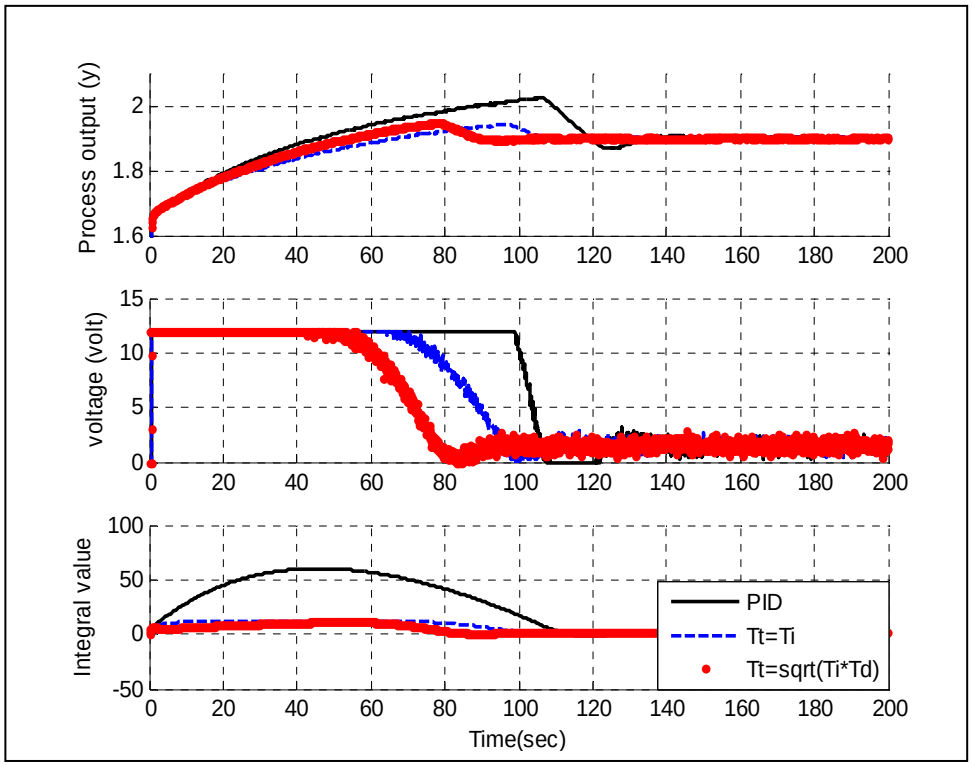


Figure20. System response, Control signal, and Integrator output for hybrid method

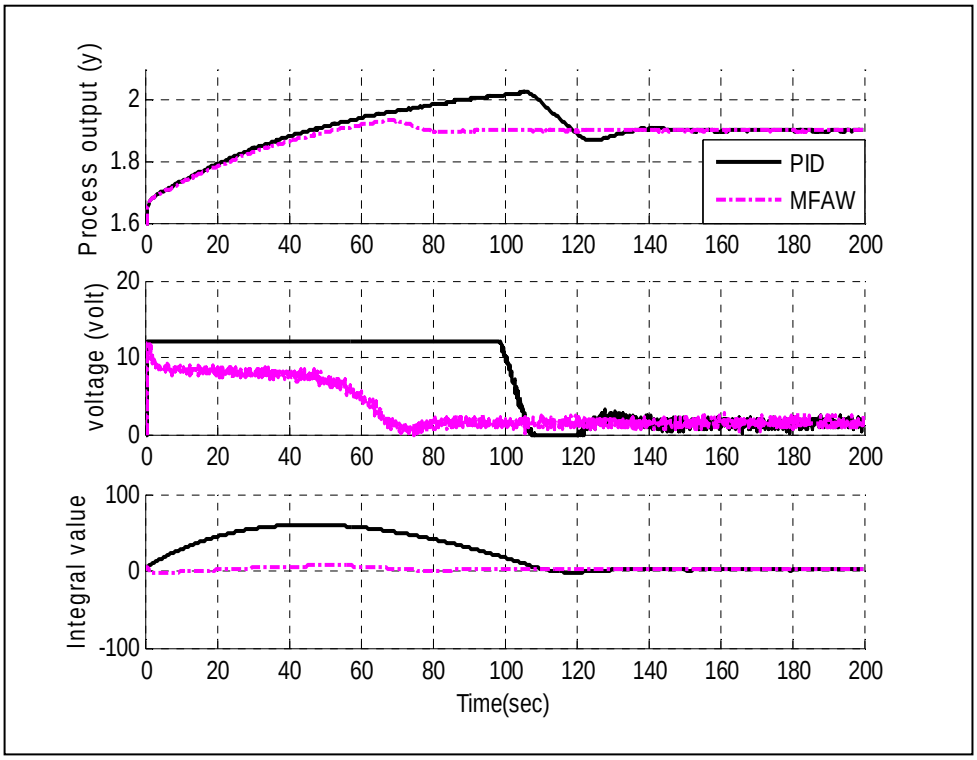


Figure21. System response, Control signal, and Integrator output for MFAW

## 7. Conclusion

PID controllers are one of the most convenient controllers utilized in industry. They can be simply tuned in order to achieve specific performance requirements, robustness and zero steady state error in the presence of constant disturbance. Applying these controllers in processes with input limitation and large set-point variation leads to an undesired phenomenon named integrator windup which yields in actuator saturation, performance deterioration, and even instability of the closed-loop system in some cases. An approximation-based AW control strategy is investigated in this paper. It has been assumed that the actuator nonlinearity can be modeled by a linear differential equation with unknown coefficients. Using Stone-Weierstrass theorem, it is verified that these differential equations are universal approximators. Experimental results evaluate the efficiency of the proposed approach. As can be seen, the controlled system comes out faster from saturation region and the reduction in settling time and overshoot are obvious. Moreover, the uniformly ultimately boundedness of steady state error is also guaranteed.

## 8. References

[1] Rehan, M., Qayyum Khan, A., Abid, M., Iqbal, N. and Hussain, B. 2013. Anti-windup-based dynamic controller synthesis for nonlinear Systems under input saturation. Applied Mathematics and Computation. 220: 382–393.

[2] Zaccarian, L. and Teel, A. R. 2002. A Common Framework for Anti-windup, Bumpless Transfer and Reliable Designs. Automatica. 38: 1735-1744.

[3] Yang, Sh-K. 2012. A new Anti-windup Strategy for PID Controllers with Derivative Filters, Asian Journal of Control. 14 (2): 564-571.

[4] Rehan, M. and Hong, K-Sh. 2013. Decoupled-architecture-based Nonlinear Anti-windup Design for a Class of Nonlinear Systems. Nonlinear Dyn. 73: 1955–1967.
[5] Ran, M., Wang, Q., Ni, M. and Dong, Ch. 2015. Simulations linear and Anti-windup controller synthesis: delayed activation case. Asian Journal of Control. 17(3): 1027-1038.
[6] Li, Y. and Lin, Z. 2016. A Switching Anti-windup Design Based on Partitioning of the Input Space. Systems & Control Letters. 88: 39–46.
[7] Zaccarian, L. and Teel. A.R. 2004. Nonlinear Scheduled Anti-windup Design for Linear Systems. IEEE Transactions on Automatic Control. 49(11): 2055-2061.
[8] Cao, Y., Lin, Z. and Ward, D.G. 2002. An Anti-windup Approach to Enlarging Domain of Attraction for Linear Systems Subject to Actuator Saturation. IEEE Transactions on Automatic Control. 47(1): 140-147.
[9] Mantz, R. J. and Battista, H. 2004. Comments on Variable-Structure PID Control to Prevent Integrator Windup. IEEE Transactions on Industrial Electronics. 51(3): 736-738.
[10] Mehdi, N., Rehan, M., Malik, F. M., Bhatti, A. I. and Tufail, M. 2014. A Novel Anti-windup Framework for Cascade Control Systems: An Application to Under Actuated Mechanical Systems. ISA Transactions. 53: 802-815.
[11] Tarbouriech, S. and Turner, M. C. 2009. Anti-windup Design: An Overview of Some Recent Advances and Open Problems. IET Control Theory and Application. 3(1): 1-19.
[12] Galeani, S., Tarbouriech, S., Turner, M. C. and Zaccarian, L. 2009. A Tutorial on Modern Anti- windup Design. European Journal of Control. 15: 418-440.
[13] Åström, K.J. and Writtenmark, B. 1984. Computer Control Systems Theory and Design, Englewood Cliffs: Prentice-Hall.
[14] Åström, K.J. and Rundqwist, L. 1989. Integrator Windup and How to Avoid it. Proceeding of the American Control Conference: 1993-1698.
[15] Kothare, M.V., Campo, P. J., Morari, M. and Nett, C. N. 1994. A Unified Framework for the Anti-windup Designs. Automatica. 30: 1869- 1883.
[16] Tyan, B., and Bernsteiu, D. S. 1995. Anti-windup Compensator Synthesis for Systems with Saturation Actuators. International Journal of Robust Nonlinear Control. 5: 521-537.
[17] Mulder, E. F., Kothare, M.V. and Morari, M. 2001. Multivariable Anti-windup Controller Synthesis Using Linear Matrix Inequalities. Automatica. 37: 1407-1416.
[18] Grimm, G., Hatfield, J., Postlethwaite, I., Teel, A. R., Turner, M.C. and Zaccarian, L. 2003. Anti-windup for Stable Linear Systems with Input Saturation: An LMI-Based Synthesis. IEEE Transactions on Automatic Control. 48: 1509-1523.
[19] Silva da., J.M.G. and Tarbouriech., J.R. 2005. Anti-windup Design With Guaranteed Regions of Stability: An LMI-Based Approach. IEEE Transactions on Automatic Control. 50: 106-111.
[20] Grimma, G., Teel, A. R. and Zaccarian, L. 2004. Linear LMI-Based External Anti-Windup Augmentation for Stable Linear Systems. Automatica. 40: 1987-1996.
[21] Walgama, K.S. and Sternby, J. 1990. Inherent Observer Property in a Class of Anti-Windup Compensator, International Journal of Control. 52: 705-724.
[22] Niu, W., and Tomizuka, M. 1998. A Robust Anti-Windup Controller Design for Asymptotic Tracking of Motion Control System Subjected to Actuator Aaturation. The 37th IEEE Decision and Control Conference. Tampa: 915-920.
[23] Hanus, R. 1980. A New Technique for Preventing Control Windup. Automatica. 21: 15-20.
[24] Hanus, R., Kinnaert, M. and Henrotte, J. L. 1989. The Conditioning Technique, A General Anti-Windup and Bumpless Transfer Method. Automatica. 21: 729-739.
[25] Hanus, R., and Peng, Y.1992. Conditioning Technique for controllers with Time Delays. IEEE Transactions on Automatic Control. 37: 689-692.

[26] Walgama, K. S., and Sternby, J. 1993. On the Convergence Properties of Adaptive Pole-Placement Controllers with Anti-windup Compensators," Journal of IEEE Transaction on Automatic Control. 38: 128-132.
[27] Zhou, Q., Shi, P., Tian, Y. and Wang, M. 2014. Approximation-Based Adaptive Tracking Control for MIMO Nonlinear Systems with Input Saturation. IEEE Transactions on Cybernetics. 45: 2119-2128.
[28] Sarhadi, P., RanjbarNoei, A. and. Khosravi, A. 2016. Model Reference Adaptive PID Control with Anti-Windup Compensator for an Autonomous Underwater Vehicle. Robotics and Autonomous Systems. Doi:10.1016/j.robot.2016.05.016.
[29] Izadbakhsh, A., AkbarzadehKalat, A., Fateh, M. M. and Rafiei, S.M.R. 2011. A Robust Anti-Windup Control Design for Electrically Driven Robots-Theory and Experiment. International Journal of Control. Automation, and Systems. 9: 1005-1012.
[30] Izadbakhsh, A. 2017. FAT-Based Robust Adaptive Control of Electrically Driven Robots without Velocity Measurements. Nonlinear Dynamics. 89: 289-304.
[31] Izadbakhsh, A., and Masoumi, M. 2017. FAT-Based Robust Adaptive Control of Flexible-Joint Robots: Singular Perturbation Approach. Annual IEEE Industrial Society's 18th International Conf. on Industrial Technology (ICIT): 803-808.
[32] Izadbakhsh, A., and Rafiei, S.M.R. 2009. Endpoint Perfect Tracking Control of Robots - A Robust Non Inversion-Based Approach," International Journal of Control, Automation, and Systems. 7: 888-898.
[33] Izadbakhsh, A. 2016. Robust Control Design for Rigid-Link Flexible-Joint Electrically Driven Robot Subjected to Constraint: Theory and Experimental Verification. Nonlinear Dyn. 85: 751-765.
[34] Visioli, A. 2003. Modified Anti-Windup Scheme for PID Controllers," IEE Proc. Control Theory and Application: 150: 49-54.
[35] Franklin, G. F., Powell, J. D. and Emami-Naeini, A. 1994. Feedback Control of Dynamic Systems, 3rd edi. Reading. MA: Addison-Wesley.
[36] Philips, C. L., and Harbor, R. D. 1996. Feedback Control Systems. 3rd ed. Englewood Cliffs. NJ: Prentice-Hall.
[37] Izadbakhsh, A. 2017. A Note on the Nonlinear Control of Electrical Flexible-Joint Robots. Nonlinear Dynamics. 89: 2753-2767.
[38] Glattfelder, A. H., and Schaufelberger, W. 1986. Start-Up Performance of Different Proportional-Integral-Anti-Windup Regulators," International Journal of Control. 44: 493-505.
[39] Astrom, K., and Hagglund, T. 1995. PID Controllers: Theory, Design, and Tuning. ISA Press, Research Triangle Park, North Carolina.
[40] Hansson, A., Gruber, P. and Todtli, J. 1994. Fuzzy Anti-Reset Windup for PID Controllers, Control Eng. Practice. 2: 389-396.
[41] de Vegte, J. V. 1994. Feedback Control Systems, 3rd ed. Englewood Cliffs, NJ: Prentice-Hall.
[42] Scottedward Hodel, A. and Hall, C. E. 2001. Variable-Structure PID Control to Prevent Integrator Windup," IEEE Trans. on. Industrial Electronic. 48: 442-451.
[43] Bohn, C. and Atherton, D. P. 1995. An Analysis Package Comparing PID Anti-Windup Strategies," IEEE Control System Magazine. 15: 34-40.
[44] Izadbakhsh, A. and. Fateh, M. M. 2014. Real-time Robust Adaptive Control of Robots Subjected to Actuator Voltage Constraint. Nonlinear Dynamics. 78: 1999-2014.
[45] Izadbakhsh, A, and Rafiei, S.M.R. 2008. Robust Control Methodologies for Optical Micro Electro Mechanical System-New Approaches and Comparison. 13th Power Electronics and Motion Control Conf, EPE-PEMC: 2102–2107.

[46] Izadbakhsh, A. and Khorashadizadeh, S. 2017. Robust Task-Space Control of Robot Manipulators Using Differential Equations for Uncertainty Estimation. Robotica. 35(9): 1923-1938.

[47] Izadbakhsh, A, and Khorashadizadeh, S. 2017. Robust Impedance Control of Robot Manipulators Using Differential Equations as Universal Approximator. International Journal of Control, doi: 10.1080/00207179.2017.1336669.

[48] Johansson, K. H. 2000. The Quadruple-Tank Process: A Multivariable Laboratory Process with an Adjustable Zero, IEEE Trans. on. Control System technology. 8: 456-465.

[49] Krikelis, N. J. 1980. State Feedback Integral Control with Intelligent Integrators, International Journal of Control. 32: 65-473.